Submitted to the Annual Review of
Physical Chemistry

LBL-7369
Preprint

COHERENT ENERGY TRANSFER IN SOLIDS

C. B. Harris and D. A. Zwemer

January 1978

Prepared for the U. S. Department of Energy
under Contract W-7405-ENG-48

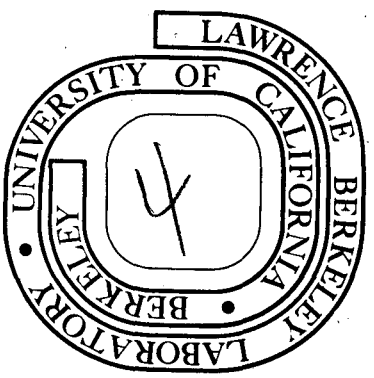

DISCLAIMER

LBL-7369

COHERENT ENERGY TRANSFER IN SOLIDS

C. B. Harris and D. A. Zwemer

January 1978

Department of Chemistry, University of California, Berkeley, California 94720 and Materials and Molecular Research Division, Lawrence Berkeley Laboratory

Send Proof to:

Prof. C. B. Harris
Department of Chemistry
University of California
Berkeley, California 94720

Work supported by the U. S. Department of Energy.

CONTENTS

INTRODUCTION

Periodicity is the property of crystalline solids that makes possible the propagation of electronic excitation in solids as coherent wavepackets in the limit of weak exciton lattice-interactions. In this review, we will briefly discuss the theoretical foundation of coherent energy migration in the various limits of the exciton-lattice interaction. In addition, we will review and evaluate experimental evidence for coherence from a variety of sources. This latter area will be the focus of this review because the experimental detection and characterization of coherent energy transfer has been a field of such great interest and moderate controversy in recent years.

In the last dozen years several general reviews on the properties of molecular solids have been published. These include those written by Hochstrasser[1], Robinson[2], Kopelman[3], and El-Sayed[4]. Soos[5] has reviewed excitation in organic-charge-transfer crystals. More recently, Silbey[6] has written an excellent review on electronic energy transfer processes in molecular crystals. Although his review has much in common with ours, he focussed on formal developments in the theory of exciton-phonon interactions while we are concerned primarily with the theory and its relation to experimental observations of coherence and exciton-phonon coupling.

While experimental evidence is of recent vintage, the prediction of coherence in molecular solids dates back to the work of Frenkel in 1931. In his original paper on excitons[7],

Frenkel develops three important insights. First, he pointed out that the electronic excitation can be delocalized and as a result be described by a series of Bloch wave-functions in analogy to the lattice modes of the crystal. Second, as a consequence of delocalization the superposition of several of the modes will form a localized wave-packet which propagates through the lattice with a group velocity determined by the exciton dispersion and the nature of exciton-lattice interaction. Third, because the excitation is coupled to the lattice, it creates a lattice distortion that travels adiabatically with the electronic excitation. As a result of these principles, a proper description of the dynamics of exciton migration in the Frenkel limit requires that the time dependence of the delocalized states of a crystal be considered. Because of the explicit localization introduced into the stationary states by phonon-exciton scattering, the electronic states, the phonon states, and phonon-exciton coupling must all be explicitly considered in terms of the crystal states. Basically, the phonons modulate the intermolecular interaction which in turn mixes the delocalized $\vec{k}$ states of the crystal and results in a state that can be described as a linear combination of the delocalized states. In the Frenkel limit, this results in a partial localization of the electronic excitation but still allows for the excitation to propagate coherently as a wave packet, provided the linear combination of $\vec{k}$ states remains unchanged for times exceeding the time associated with the nearest-neighbor electronic intermolecular

exchange. Indeed, it is the average frequency at which the linear combination of $\vec{k}$ states changes relative to the intermolecular interaction time that determines the dominant mechanism responsible for electronic energy transfer in solids at both high and low temperatures.

Although the number of different operational definitions of coherence is large, they may be broadly categorized into two groups. In the first, the stationary state of the excitation is a delocalized state or a wavepacket of states characterized by a constant wave-vector and group velocity. The wave-vector $\vec{k}$ is a good quantum number for times longer than the intermolecular transfer time. The extent of coherence determines the k-state lifetime and as a result, the homogeneous lineshape function for absorption to the exciton band edge. The implications of coherence in spectroscopy from this point of view have been developed and refined by a variety of people including Toyozawa[8-11], Sumi[12,13], Suna[14], Harris[15,16] and others[17-20], who have calculated optical absorbtion lineshapes for exciton transitions in various limits. This also provides the rationale behind the experimental lineshape studies described later in this review, Toyozawa's analysis[8] for alkali halide absorbtion spectra, and Thomas and Hopfield's demonstration of exciton coherence in CdS[21]. In addition, this description of coherence provides a means for easily relating the exciton's coherence time to the correlation time of a

variety of other experimental techniques such as ESR and NMR. It was on this basis that coherent migration in triplet exciton bands in molecular solids was established by Harris and coworkers[16,22-24].

A second and more empirical definition is that a coherent exciton has a mean free path greater than one lattice site but its motion is described by random walk processes on some time scale longer than the intermolecular transfer time. Studies of exciton dynamics based upon a statistical model for the probability of trapping excitons in the coherent and random walk limits relies on this definition. Implicit in these studies is a detailed consideration of the energy dispersion of the band, the number of k states comprising the band, and the partitioning of energy between the band and trap states when a Boltzmann distribution characterizes the ensemble. Exciton diffusion constants have been measured experimentally and used to infer properties of coherence based on this definition. The early work of Gallus and Wolf[25] in phenanthrene and Kepler and Switendick[26] and Avakian and Merrifield[27] can be interpreted in this context.

There is no contradiction between these two concepts of coherence although we feel the first definition can be correlated better with theory. Under the assumption of first-order stochastic Markoffian scattering, where the probability of exciton scattering is independent of previous scattering events, the k-state lifetime, $\tau(k)$, and the exciton mean free

path, $\ell(k)$, are simply related by the group velocity.

$$\ell(k) = \tau(k)\, V_g(k) \qquad (1)$$

Each experiment used to measure coherence has a different time scale associated with it and thus the imposed time scale determines whether the exciton looks coherent or diffusive with a given method. To illustrate these principles more quantitatively, we will begin our discussion with the description of the theory of coherence for a two-molecule system (dimer) and extend the concepts to a one-dimensional linear exciton band.

EXCITON THEORY AND COHERENCE

Consider a system of two identical molecules in an inert lattice. This system has two excited states, state $|1\rangle$ in which molecule 1 is excited and molecule 2 is in the ground state, and state $|2\rangle$ in which the excitation is on the other molecule. In second quantized form, the Hamiltonian for this system is

$$H = E_o(a_1^+ a_1 + a_2^+ a_2) + V(a_1^+ a_2 + a_2^+ a_1) \qquad (2)$$

where E_o is the excited state energy for the isolated molecule and operations a_i^+ and a_i create and destroy the excitation on molecule i. V represents an interaction between the electrons of the two molecules and is generally separated into a Coulomb and an electron exchange term.[28]

$$V = J - \beta \qquad (3)$$

J, the Coulomb contribution, accounts for the electron-electron repulsion and predominates in the interaction of singlet states, but $J \to 0$ for triplet-singlet coupling and β, the exchange integral, becomes responsible for triplet dimer splitting.

The degenerate states $|1\rangle$ and $|2\rangle$ are nonstationary states of the system. If the excitation rests on molecule 1 at some initial time, it may be shown[6] that the probability of being on molecule 2 at some later time t is

$$P_2(t) = \sin^2 Vt/h \qquad (4)$$

The excitation oscillates coherently between molecules 1 and 2 indefinitely in the absence of a coupling to the lattice. Since the intermolecular transfer time is one-fourth of the period of oscillation, the phase of oscillation or the phase of the time-dependent stationary state is retained for a much longer period of time than the intermolecular transfer time. In this case, the dimer is said to be coherent. The stationary states of the system are the symmetric and antisymmetric superpositions of the two molecular states

$$\psi(\pm) = 2^{-1/2}\left[|1\rangle \pm |2\rangle\right] \qquad (5)$$

and are split by 2β

$$E(\pm) = E_o \pm \beta \qquad (6)$$

The fact which should be self-evident is that the dimer states $\psi(+)$ and $\psi(-)$ which contain the well-defined phases are not necessarily coherent for an infinite time because of the interaction between the dimer states and the environment via a relaxation Hamiltonian. Coherence in the dimer states is established by the relative lifetime of the state, $\psi(+)$ or $\psi(-)$, compared to the resonance transfer time whose frequency is 1/h times the separation between the two levels, 2β. In effect, one must experimentally determine whether the lifetime of the phase, $\tau(+)$ and $\tau(-)$ for the plus and minus states, respectively, is longer or shorter than $h/2\beta$.

If $\tau(\pm) < h/2\beta$, the states are incoherent and possibly indistinguishable. On the other hand, if $\tau(\pm) > h/2\beta$, say, approaching the radiative lifetime of the species, the dimer is coherent because there has not been an energy fluctuation during that time period, and hence the phase of the wavefunction is well-defined from the initial time, t=0, the time at which the excited state is created. Coherence times are determined by fluctuations of the off-diagonal matrix elements of the time-dependent density matrix when the stationary states are solutions to the zero order Hamiltonian matrix responsible for dimer splitting[29-32].

The properties of one-dimensional excitons in the absence of lattice coupling are exactly analogous to the dimer system. A finite linear array of N independent identical molecules

has N degenerate electronic states. The energy, E_o, of this system corresponds to the excited state energy of a single molecule. If the molecules interact pairwise, the Hamiltonian of the system becomes

$$H = \sum_{n=1}^{N} E_o \, a_n^+ a_n + \sum_{n,m}^{N} \beta_{nm} \, a_n^+ a_m \qquad (7)$$

The stationary eigenstates of the Hamiltonian are the delocalized Bloch wavefunctions

$$|k\rangle = N^{-1/2} \sum_{N} e^{ik \cdot r_n} |n\rangle \qquad (8)$$

characterized by the exciton wave-vector $\underline{k}$. In one-dimensional systems with only nearest-neighbor interactions, the exciton dispersion is

$$\epsilon(k) = E_o + 2V \cos k a \qquad (9)$$

where a is the intermolecular spacing. The properties of the one-dimensional dispersion are summarized in Fig. 1.

In order to properly consider exciton migration in solids, one must introduce exciton-phonon coupling which modulates the intermolecular interaction and mixes the delocalized k-states. Phenomenologically, this partially localizes the

the exciton but still allows it to propagate coherently as a wave-packet, provided the explicit linear combination of k-states remains unchanged for times exceeding the time for nearest neighbor resonant transfer.[33] For coherent propagation to be a meaningful concept, the wavepacket uncertainty in position, Δr, must be smaller than the exciton mean free path, setting a minimum width to the distribution of k-states in the wave packet.

$$\Delta k \geq (\Delta r)^{-1} \tag{10}$$

In such a case, the Frenkel exciton propagates coherently with a group velocity characteristic of its energy and the linear combination of k states

$$V_g(k) = \frac{1}{\hbar} \left(\frac{\partial \varepsilon(k)}{\partial k}\right) \tag{11}$$

which becomes, for the one-dimensional case,

$$V_g(k) = \frac{2\beta a}{\hbar} \sin k a \quad . \tag{12}$$

This is peaked for k-states in the center of the band as shown in Fig. 1. The average group velocity at a given temperature, $\langle V_g(T) \rangle$, is given by the normalized sum over the velocities of the k states in the band, with each velocity weighted by the probability of finding the system in that k-state

under Boltzmann equilibrium.[34]

$$\langle V_g(T)\rangle = \frac{2Va}{h} \sum_k \sin ka \; e^{-2V \cos ka/k_bT} \Big/ \sum_k e^{-2V\cos ka/k_bT} \tag{13a}$$

Restricting the summation to $k > 0$ states to obtain an average scalar velocity, (10a) converges for large N to

$$\langle V_g(T)\rangle = (2Va/h)\,(2k_bT/\pi V)^{1/2}\,[I_{1/2}(Z)/I_o(Z)] \tag{13b}$$

where

$$I_o(Z) = \frac{1}{\pi} \int_o^{\pi} e^{Z \cos\theta} d\theta \tag{13c}$$

$$I_{1/2}(Z) = (\tfrac{1}{Z}/\pi)^{1/2} \int_o^{\pi} e^{\pm Z \cos\theta} \sin\theta \; d\theta \tag{13d}$$

The average intermolecular transfer time is given by the average group velocity and the lattice spacing

$$\langle\tau\rangle = a/\langle V_g(T)\rangle \tag{14}$$

The complete Hamiltonian for an extended system[6] including coupling to the lattice is

$$H = \sum_n E_o a_n^{+} a_n + \sum_{n,m} V_{nm}\, a_n^{+} a_m + \sum_{n,q} \omega_q \,(b_{qn}^{+} b_{qn} + \tfrac{1}{2}) + \sum_{n,q} g_{nq}\, a_n^{+} a_n \,(b_{qn}^{+} + b_{qn}) + \sum_{n,q} h_{nq}\, a_n^{+} a_n \,(b_{qn}^{+} + b_{qn})^2 \tag{15}$$

where ω_q is the energy of phonon q, and g_{np} and h_{np} represent the linear and quadratic exciton-phonon coupling constants, respectively. Theoretical studies of localization and coherent migration based on solutions to the above Hamiltonian have been given by a variety of workers and has been reviewed extensively and with great clarity by Silbey[6].

It should be noted that each of the principal theoretical formulations, apart from Förster's study of incoherent transfer[35], contain a coherent component in the transport equations that persists to relatively high temperatures. The Haken-Strobl-Reinecker[36-38] model requires no specific information on exciton-phonon coupling, but instead makes the site and interaction energies (E_o and V_{nm} in eq. 15) time-dependent, fluctuating stochastically with delta function auto-correlation times (Markov limit). The expression they derive for the diffusion constant contains an incoherent term determined by the fluctuation amplitude and a coherent term which goes to infinity in the limit of zero fluctuation amplitude. Grover and Silbey[39,40] begin with a dynamical model of the lattice coupling and transform to operators creating and destroying excitons with associated phonons. To obtain analytical expressions for exciton mobility, they also make the Markov scattering assumptions and get a diffusion constant similar to that of Haken and

co-workers. Munn and Siebrand[41] have pointed out the importance of the quadratic coupling terms which were neglected by Grover and Silbey. Using generalized master equations, Kenkre and Knox[42-45] have derived the time evolution of an exciton system without the Markoffian assumption, permitting the use of non-exponential coherence memory decays. These authors have also investigated the transition from coherent to Fermi golden rule intermolecular transfer rates that accompanies increased phonon scattering.

Theoreticians have also considered coherence in substitutionally-disordered systems containing traps and barrier states in the chain. Pearlstein and collaborators[46,47] calculated the quenching kinetics in finite chains with energy traps, finding that fully coherent excitons have low probability amplitudes at the traps and are quenched more slowly than their group velocity along the chain would indicate. Greer,[48,49] on the other hand, investigated the exciton flux through a region of a linear chain containing N barriers to scatter the excitons. He found that transfer through this region is coherent, i.e., the flux is independent of N, only for a periodic distribution of barriers. Even for random barrier placement, however, the Frenkel exciton flux does not show pure diffusional behavior. Zwemer and Harris[50] consider coherent exciton quenching in a system with traps and barriers, and report a transition from diffusional to coherent transport on the macroscopic level with increasing barrier transmission coefficient.

For the remainder of this review we will concentrate on how exciton scattering affects various experimental observations in

the limit of stochastic Markoffian scattering. In such cases, the processes may be described by simple time-independent rates for transfer between k states or between the $\psi(+)$ and $\psi(-)$ states of the dimer. Each k-state has a lifetime, $\tau(k)$, limited by the scattering rates to other k' states, $W_{kk'}$, and the radiative or non-radiative lifetime of the excitation, τ_L;

$$[\tau(k)]^{-1} = \sum_{k'} W_{kk'} + [\tau_L]^{-1} \qquad (16)$$

An exciton with wave-vector k may be considered coherent if $\tau(k)$ is greater than the intermolecular transfer time, as given by eq. 14.

THE DETERMINATION OF COHERENCE USING ELECTRON SPIN RESONANCE.

The single system which has received the greatest amount of attention as an example of coherent transfer in molecular solids has been 1,2,4,5-tetrachlorobenzene (TCB). The space group for TCB is $P2_1/c$, with two molecules in the unit cell.[51] A phase transition at 188°K changes the lattice into a triclinic space group, but the structure of the latter is closely related to the room-temperature crystal structure in molecular orientations and unit-cell dimensions. The stacking of the translationally equivalent molecules is along the $\vec{a}$ crystallographic axis in both phases, monoclinic and triclinic. Figure 2 illustrates the nature of this stacking. The out-of-plane molecular axis is almost parallel

to the axis $\vec{a}$. This fact, together with the small length of $\vec{a}$ compared to the $\vec{b}$ and $\vec{c}$ lattice constants, gives its one-dimensional character. Because of the structure, the exchange interaction for the triplet state is largest along the $\vec{a}$ axis. In cases where the exchange interaction is along translationally equivalent molecules in the unit cell, the triplet band structure of the crystal consists of three parallel bands each split in first order by the electron spin dipolar interactions. In second order, however, the effect of spin-orbit coupling gives rise to an anisotropy in the zero-field splitting across the band from k = 0 to the k = $\pm$ π/a.[24,33] As a result, a k-dependent zero-field splitting exists between any two spin sublevels and a manifold of ESR transitions are allowed, each associated with the individual k states in the exciton band.

The proper representation in terms of the Bloch formalism[52] in the absence of spin averaging between k states (i.e., no phonon-exciton scattering) is a set of Bloch equations, one for each k state in the band. In the rotating frame in the presence of a weak oscillating field of the form

$$H(t) = -\gamma H\beta \cos \omega t \qquad (17)$$

the in-phase, u, and out-of-phase, v, components of a complex moment are definable as

$$G = u + iv \qquad (18)$$

Representing ω as the applied microwave frequency and ω_o^k as the resonant microwave frequency associated with the spin sublevels of the k^{th} state in the band, the complex moments obey the following Bloch equations (one equation for each k state in the exciton band).

$$\frac{dG_k}{dt} + \frac{1}{T_2(k)} - i\,(\omega_o^k - \omega) \quad G_k = -i\,\gamma\, H_1\, M_o^k \qquad (19)$$

M_o^k should be related to the exciton density of states and the Boltzmann factor in the exciton band

$$M_o^k = C_{mn} \cdot D(\varepsilon)\, e^{-\varepsilon(k)/K_B T} \qquad (20)$$

C_{mn} is a constant related to the spin alignment in the m^{th} and n^{th} spin sublevels which are being coupled by the microwave field; $D(\varepsilon)$ is the density of states function for the exciton band; and $\varepsilon(k)$ is the energy dispersion of the triplet band. The weak field modified (2k + 1) Bloch equations in steady state are:

$$(1/T_2)G_k - i(\omega_o^k - \omega)G_k = -i\,\gamma\, H_1\, D(\varepsilon)\, e^{-(k)/K_B T} \cdot C_{mn} \qquad (21)$$

Averaging effects on the microwave transitions in the exciton spin manifolds are expected to contribute to the line shape function

when exciton-phonon scattering results in a change of k state on a time scale comparable to the differences in Larmor frequencies associated with the initial and final exciton k states between which scattering has occurred. The effects of phonon-exciton scattering can be incorporated into the modified Bloch equations through a scattering matrix which completely spans the basis states of the Frenkel excitons. Assuming that the spin-phonon coupling is negligible in the phonon-exciton coupling channels, the modified 2k + 1 Bloch equations can be written as

$$(1/T_2)G_k - i(\omega_o^k - \omega)G_k = -i\,\gamma\, H_1\, D(\varepsilon)\, e^{-\varepsilon(k)/kT}.\; C_{mn} \qquad (22)$$

$$+\sum_{k'}\left[G_{k'}/\tau_{k'k} - G_k/\tau_{kk'}\right]$$

where $\tau_{kk'}$ represent the exciton-phonon scattering times. The formulation of eq.22 assumes that the averaging of the Larmor components ω_o^k via phonon-exciton scattering is a stochastic Markoffian process. In the limit that $\tau_{kk'} \to \infty$ for all values of the wave vector k, eq.22 represents (2k + 1) independent linear equations whose imaginary components represent Lorentzian absorption curves, each centered at ω_o^k with a line width related to T_2. This is termed slow exchange. In zero field, the area under each transition is proportional to the density of exciton states times the Boltzmann factor evaluated at $\varepsilon(k)$ in the triplet exciton band. The lineshape function for the electron spin resonance band-to-band transition is expected to be simply the weighted

sum of the independent Lorentzian lines each centered at the appropriate ω_o^k, i.e.,

$$g(\omega) = \frac{\delta}{\pi} \int_0^{\pi/a} \frac{\exp \Delta_T(1-\cos ka)/K_B T}{[\omega + \Delta_{ST}^{\xi} \cos ka]^2 + [\delta^2]} dk \qquad (23)$$

$2\Delta_T$ is the one-dimensional triplet band dispersion and equal to four times the effective intermolecular exchange interaction, K_B is the Boltzmann constant, T is the temperature, Δ_{ST}^{ξ} is a reduction factor related to spin orbit coupling with excited singlet states, and δ is the half width at half height of an individual k state transition whose homogeneous line width is related to T_2.

The essential features of the EPR transitions are: (a) the frequencies of the zero-field electron spin transitions are related to both the anisotropy of the spin-orbit coupling in the first Brillouin zone and the zero-field spin dipolar Hamiltonian; (b) the intensity of the ESR transitions are related to the density of states function and therefore the effective intermolecular exchange interaction can be obtained experimentally; and finally, (c) the lineshape function gives a measure of phonon-exciton scattering processes and thus the coherence lifetime of the individual k states in the band can be determined when the system is in slow exchange. Moreover, the theory and experiments are easily adaptable to dimer and n-mer dispersions in a straight forward manner.

The same treatment for the symmetric and anti-symmetric states of the dimer shows that the relationship between the exciton spread in Larmor frequency and the dimer spread $[\omega(+)-\omega(-)]$ is:

$$[\omega(+)-\omega(-)] = \frac{1}{2}[\omega(k=0) - \omega(k= \pm \pi/a)] \qquad (24)$$

Physically, this is because the dimer splitting, 2β, is half the total band width, 4β, for a one-dimensional exciton. As a result, the k-dependent spin-orbit perturbation in the exciton is reduced by a factor of two for a two-molecule chain. Furthermore, the monomer EPR frequency should be at $k = \pm \pi/2a$ (the center of the band). These coherent properties for excitons are all conceptually related to the coherent properties of dimers; $\tau(k)$ is related to $\tau(+)$ and $\tau(-)$ for the two dimer states, and $\ell(k)$ is some number of lattice spacings the exciton propagates before scattering, while the dimer equivalent is the distance between the interacting molecules of the pair. The lifetimes of the plus and minus states of a dimer in a host lattice (characterized by k_n band states) are given by

$$\left[\tau(\pm)\right]^{-1}_{lat} = (\tau(\pm))^{-1} + \sum_{k'_n} (\tau_{k'_n})^{-1} = \Gamma(\pm). \qquad (25)$$

In the zeroth-order approximation the uncertainty width is the same for both the plus and minus states,

$$\Gamma(\pm) = \Gamma = (\tau)^{-1}. \qquad (26)$$

Figure 3 shows the experimental observables for coherent dimers.

For an exciton, a sum over all k states of the band must be carried out. In the zeroth-order approximation,

$$\Gamma(k) \equiv [\tau(k)]^{-1} = \sum_{k'} (\tau_{kk'})^{-1} \quad . \qquad (27)$$

$\tau_{kk'}$ is the probability that an exciton initially in an energy associated with the kth state is scattered to a final energy with the state k'. The relationship between $V_g(k)$ and the band dispersion for excitons is given in figure 1 which should be compared with the dimer coherent parameters given in fig. 3 The experimental observations which are necessary to establish coherence in either the dimer or exciton case must establish the existence of separate transitions for the individual k states of the band or the $\psi(+)$ and $\psi(-)$ states of the dimer. In the limit where the exciton or (dimer)-phonon scattering time is longer than the reciprocal of the difference in the Larmor frequencies the spin can absorb the rf fields in each state of the dimer or in each state of the exciton. On the other hand, fast scattering leads to a collapse of the resonance absorption into one line centered around 1/2 $[\omega(+)+\omega(-)]$ for the dimer or at the center of the band for the exciton. This is illustrated in figure 4 . Coherence in triplet excitons was first established in TCB by Francis and Harris[22-24] by monitoring the optically-detected ESR band-to-band transition in the lowest triplet state at 3.3°K. The observed lineshape of the D-|E| transition

is shown in figure 5. It appears much like the one-dimensional system of fig. 3. The theoretical fit gives a k-state lifetime greater than 10^{-7} seconds, which is much longer than the intermolecular transfer time, 10^{-11} seconds. They established that the exciton bandwidth, the minimum coherence time and the density of states function in the band could be obtained from zero field optically detected magnetic resonance at liquid He temperatures. In addition, they established that all k states have about the same coherence lifetime, implying the lack of strong k dependent phonon-exciton scattering at 4.2 K. If localization of the band states via mixing of the + and - wave vector states (elastic damping) is less than localization via inelastic processes such as phonon-exciton scattering, a coherence time of 10^{-7}s could allow coherent exciton migration to propagate as far as 10^{4}Å for states in the center of the band ($k=\pm\pi/2a$) in these crystals. On the other hand, resonant scattering or damping could greatly reduce this coherence length. Unfortunately, the Larmor frequencies for +k and -k states, $\omega_o{}^{k}$ and $\omega_o{}^{-k}$, are the same, and hence, the above experiments cannot detect the effects of resonant scattering or damping. From other experiments,

however, a lower limit on the coherence length in these crystals for $k = \pm \pi/2a$ of 300 Å -400Å has been determined.[53,54]

The coherent nature of dimer transfer was first established by Zewail and Harris[29,55-56] also using optically detected electron spin resonance in the lowest triplet state of 1,2,4,5-tetrachlorobenzene. The dimer observed is the translationally equivalent pair along the $\vec{a}$ axis embedded in a deuterated solid. The coherent states of the dimer are the symmetric and antisymmetric linear combinations of the individual molecule excited states and are split by 2β as discussed in eq. 5 and 6 . Only one dimer state has oscillator strength to the ground state in optical absorbtion, but spin-orbit coupling between the observed triplet sublevels and higher singlet states maps out the dimer splitting onto the ESR spectrum so that the $\psi(+)$ and $\psi(-)$ components of the ESR transition have different frequencies.

In 5% h_2-TCB in d_2-TCB, two peaks ascribed to the dimer transition flanking each monomer transition are resolved. The assignment is supported by the concentration dependence, saturation power dependence, and Boltzmann distribution of the dimer peak intensities. Because the two dimer peaks can be resolved, the system must be in slow exchange where $W_{\pm} < \delta\omega$ or $\tau(\pm) > (\delta\omega)^{-1}$. This sets a minimum coherence lifetime of 5×10^{-7} sec, which is $\sim 10^4$ greater than the intermolecular transfer time of 10^{-11} sec. The excitation

oscillates coherently many times between the dimer molecules before scattering to the other dimer state.

In view of the importance of the exciton band-to-band line shape broadening function in the interpretation of properties associated with coherent energy migration in triplet excitons, it is desirable to have an experimental method capable of investigating the homogeneous character of the electron spin transitions. The homogeneous line width can be directly related to the lifetime of the states when other contributions to the line width, such as fluctuating local fields, are negligible compared to uncertainty broadening. The experimental techniques should allow the full correlation function for the dynamical processes to be obtained. Most of these requirements are satisfied by optically detected electron spin coherence techniques[57,58], such as the electron spin echoes in which the Fourier transform of the decay of the echo measured as a function of the time (2τ) between microwave pulses is related to the lineshape function for the phonon-exciton processes which dephase the spins. Recently, in an important experiment, Botter, Dicker, and Schmidt[59] monitored the ESR linewidth of TCB upto 15°K using two-and three-pulse spin echoes. Spin echoes, which do not appear above 2.2°K, show a constant memory dephasing time below 1.6°K that the authors ascribe to impurity and trap scattering. More importantly, however, the spin echo

technique has a variable correlation time determined by the pulse spacing, so an estimate of the wave vector change may be made. The authors report that scattering in the coherent regime of TCB involves k-state changes of less than a MHz, much smaller than the total linewidth. The ODMR studies also show the double maximum band-to-band transition at 4.2°K changing to a symmetric Lorentzian at the center of the band at 8°K as predicted by Harris et al.[33] This is precisely what is expected when the system proceeds from a slow exchange region to fast exchange with increasing temperature.

Other systems have also been studied. Botter, Nonhof, Schmidt, and Van der Waals[60] measured the coherence time of translationally inequivalent naphthalene dimers in perdeutero-naphthalene using both zero-field ESR techniques and electron spin echoes. The Davydov splitting of 2.5 cm^{-1} in the optical spectrum of the dimer shows a coherence time $>10^{-11}$ sec. In zero field ESR, $\psi(\pm)>$ transitions are split by ten megahertz, corresponding to a minimum coherence lifetime orders of magnitude longer. By monitoring the frequency shift with temperature in the zero field splittings and the temperature-dependent contribution to the homogeneous linewidth measured by spin echoes, lifetimes in both states can be derived. The system shows maximum linewidth about 1.7°K, corresponding to intermediate exchange but shows coherent behavior at lower temperatures.

Schmidberger and Wolf[61] have extensively investigated the behavior of the conventional and optically detected ESR lineshapes of a second system, 1,4-dibromonaphthalene. The microwave saturation behavior of the transition shows some departure from complete homogeneity,[61c] so no exact value for the coherence time of the k-state is available. However the temperature dependence of the lineshape[61b] is constant at low temperatures, rises as the temperature cubed to a maximum at 16 K, and then decreases asymptotically to a constant room temperature value. The low temperature behavior of the exciton is characterized as coherent by the definition of Haken and Strobl[62]

$$\gamma_o \leq 2\beta \qquad (28)$$

where γ_o, the local site energy fluctuation, has an upper limit set by the observed linewidth. The T^3 dependence is attributed to dephasing by scattering with acoustic phonons, whose population density goes as T^3 in a Debye solid. Above 16 K, the exciton motion is incoherent and the lineshape is motionally narrowed. Schmidberger and Wolf also show that the low-temperature coherence is limited by exciton transfer between magnetically inequivalent chains.[61d] This cross-chain hopping rate, measured in another series of experiments, puts an upper limit on the coherence time of 10^{-8} sec.

OPTICAL LINESHAPE STUDIES

The demonstration of exciton coherence by analysis of the optical absorbtion lineshape has been hampered by two problems, one experimental and one theoretical. Experimentally, inhomogeneous broadening of the observed transition by crystal defects, internal strain, and the distribution of chain lengths in one-dimensional systems is a recurrent problem in molecular crystals at low temperatures. This can be circumvented by careful observation of the temperature dependence of the linewidth and optical coherence techniques[63] hold promise for future work. On the other hand, the interpretation of lineshape functions has been hampered by the lack of a commonly accepted model for the effects of exciton-phonon coupling and coherence on the k=0 state observed in optical absorbtion and emission although many models have been proposed, beginning with Davydov[17] and Rashba[18]. With this in mind, we will review the predictions and regions of applicability of those models most widely used.

Given complete knowledge of the wave function and energy level structure of the exciton bands and the exciton lattice Hamiltonian, Toyozawa's lineshape model predicts a Lorentzian for weak exciton-phonon coupling and a Gaussian for strong coupling.[8-11] The strength of coupling is determined by the relative magnitude of exciton bandwidth and exciton-phonon coupling constants, so that the weak coupling limit is roughly

synonomous with the limit of coherent exciton propagation. Toyozawa's model has the advantage of extreme generality and has been used to predict the behavior of semiconductor and ionic solids as well as organic insulators. It does not apply, however, in the low temperature limit when the k=0 absorbtion is at the edge of the exciton band, as in one-dimensional systems. More significantly, the model is extremely difficult to invert. Given the phonon energies and scattering rates, it is straightforward to calculate the lineshape but it is very difficult to extract energies and rates from an experimental lineshape.

This difficulty has been illustrated by Burland, Cooper, Fayer, and Gochanour,[64] who report the singlet-triplet absorbtion lineshape of TCB between 2K and 45 K. The lineshape changes from an asymmetric Lorentzian at low temperature to a symmetric Lorentzian about 14 K and finally to a symmetric Gaussian above 20 K. The asymmetry of the initial lineshape reflects the position of the k=0 state at the top of the band. As the temperature increases, exciton-phonon scattering mixes dipole intensity into all the k-states and the absorbtion maximum shifts to give a symmetric Lorentzian at the center of the band. The authors ascribe the final transition to a Gaussian lineshape to the localization of the exciton. While this behavior qualitatively matches the Toyozawa predictions, the model's temperature dependence is too complex to extract

scattering rates and coherence lifetime from the experimental lineshape data.

The difficulty has been circumvented somewhat by Morris and Sceats,[65-67] whose model enjoys the advantage of easy comparison with experiment. Using the Green's function approach to lineshape initiated by Davydov[17] and others, Morris and Sceats have directly and simply defined the moments of the optical transition in terms of the dynamical scattering rates and energies in each of several limiting regimes: weak coupling, strong coupling, and polariton-phonon coupling. The model assumes a Lorentzian lineshape for the transition and, in the weak coupling limit, predicts increasing second and third spectral moments with increasing temperature.

The model was developed to analyze reflection spectra of strong singlet exciton absorbtions over a very wide temperature range and the question of exciton coherence was not of primary concern to the authors. The high temperature behavior is confused by the presence of multiple scattering mechanisms and "average" values of phonon energy and scattering rate are extracted. The exact application of the theory to a particular scattering mode at low temperatures is largely untested, although the authors do briefly consider the exciton coherence length in the 4000 Å anthracene singlet band, for which weak coupling holds. They report that the exciton mean free path may be as much as 20 Å , depending on the average group velocity.

Haken and Reinecker[37,38] and Sumi[12,13] start with Hamiltonians that do not include separate dynamical terms for phonons and exciton-phonon coupling. Instead, these models allow the molecular site (on-diagonal) energy and intermolecular interaction (off-diagonal) to fluctuate according to stochastic Gaussian and Markoffian processes, and solve for the optical linewidth in terms of the fluctuation correlation times. Haken and Reinecker predict a Lorentzian lineshape which broadens with increased fluctuation rate. Sumi discards the off-diagonal fluctuation in the intermolecular interaction β and separates the on diagonal autocorrelation function into a coupling strength D and a dephasing rate γ, and solves for the lineshape using the coherent potential approximation.[68] The three limits of the Sumi model are (i) $\beta >> D, \gamma$ where the lineshape is Lorentzian in the weak coupling limit; (ii) $\gamma >> D, \beta$ where the phonon energy is so rapidly exchanged between sites that the lineshape is a motionally narrowed Lorentzian; and (iii) $D >> \beta, \gamma$ where the strong coupling limit gives a Gaussian lineshape.

Both models readily give exciton mean free path lengths on the basis of experimental lineshapes. Sumi demonstrates that a coherent component remains in the exciton propagation rate for the singlet and triplet excitons in anthracene as high as 100 K. The nature of the models do not allow analysis in terms of a specific scattering mechanism.

Using a different approach, Harris[15] has explicitly related the optical lineshape function to k-scattering via exchange

69-72
theory, under the assumption that the dominant dephasing mechanism for the electric dipole transition to the k=0 state results from the absorbtion and emission of a phonon. This dynamical model assumes that exciton is scattered to an entirely different k state and that the dephasing of the optical absorbtion comes about via frequency differences of the phonon in the ground and excited state. Phonon energy exchange modulates the transition dipole moment through the quadratic terms of the exciton-phonon coupling in this model and exchange averaging is treated as a stochastic process and is related to the time-independent phonon promotion and relaxation rates which introduce a random frequency modulation into the electric dipole auto-correlation function.

The Harris exchange model makes several distinctive predictions. The manifestation of exchange is to produce both a temperature dependent line broadening and frequency shift when the difference between the ground and excited state phonon energies, $\delta\omega$, and the lifetime of the exciton-phonon complex, τ , satisfy the condition of intermediate exchange

$$\delta\omega\ \tau \sim 1. \qquad (29)$$

In essence, the lifetime τ in the excited phonon state must be long enough to partially dephase the correlation function for the transition dipole to k=0, but short enough to bring back phase memory of the upper state frequency. If the phonon's

energy is lower (higher) in the excited state than in the ground state, the frequency shift is to lower (higher) frequency with increasing temperature. The model predicts a Lorentzian lineshape for $\omega \cong \omega_o$, the transition frequency without exchange. The same lineshape function has been derived for several exchange theories in magnetic resonance.[70-72] Most importantly, under the condition of intermediate exchange, it is possible to extract the energy of the scattering phonon and the phonon promotion rate which limits exciton coherence from the temperature dependence of the experimental lineshape and frequency shift.

The exchange model gives the exciton-scattering rate for a particular phonon mode in a computationally and conceptually simple way; however, the interpretation of the lineshape function in terms of the exciton coherence can only be valid when it can be shown that the scattering rate from the observed mode dominates all others at a particular temperature. The model is primarily applicable to low temperatures where few modes are populated.

The exchange model has been applied by Harris[16] to the question of coherence in the linear exciton system 1,4-dibromonaphthalene (DBN). The work of Burland[73] and Burland, Konzelman, and Macfarlane[74] in this system has established that (i) the triplet exciton absorbtion linewidth for both crystal sites in DBN broadens in a non-exponential manner from 4 K to 40 K, (ii) the lineshape changes from an asymmetric Lorentzian to a symmetric Lorentzian between 5 and 25 K, and (iii) both transitions are frequency

shifted to lower energy with increasing temperature. Analyzing only the linewidth and not the frequency shift, Burland, Konzelman and Macfarlane[74] are unable to distinguish between the alternative one and two phonon scattering mechanisms they propose. Using this data, Harris has presented an analysis of the optical lineshape based on exchange.[16] Noting that the ratio of the temperature-dependent portion of the frequency shift Δ_{eff} and the linewidth T_{eff}^{-1} is equal to

$$T_{eff}^{-1}/\Delta_{eff} = \delta\omega\tau, \qquad (30)$$

this ratio plotted against temperature for both the absorbtion origins in the DBN triplet exciton spectrum gives a constant average value of 0.63 for site I (20,192 cm^{-1}) and 0.75 for site II (20,245 cm^{-1}). Having established that intermediate exchange holds, Harris obtains quantitative estimates of τ and $\delta\omega$. The observed k=0 state lifetime is 2×10^{-7} sec. and 3.3×10^{-6} sec. at 4 K and 1.4×10^{-12} sec. and 2.5×10^{-12} sec. at 30 K for sites I and II respectively, which values are all longer than the intermolecular transfer time, 7×10^{-13} sec. The energies of the scattering phonon modes are 38 cm^{-1} and 45 cm^{-1} for the two sites.

EXPERIMENTAL TECHNIQUES BASED ON ENERGY DISTRIBUTION FUNCTIONS.

Exciton mean free path measurements have been less successful in demonstrating exciton coherence in many cases than lineshape interpretation. A coherent exciton has a mean free path greater than the intermolecular spacing and as such the extent of coherence determines the path length. These measurements require the detection of exciton transfer between spectroscopically distinguishable initial and final states. A distinction between coherent and incoherent migration is often made in assessing whether or not a dynamical model provides a mechanism for achieving thermal equilibrium between these states within the lifetime of the state. Usually the experiment measures energy partitioning between an exciton band and traps, the time-dependence of emission build-up and decay in band or trap, or triplet-triplet exciton annihilation. In practice, these often require the introduction of isotopic, chemical, or structural traps or barriers outside the exciton band. Unfortunately, transfer processes associated with two or more component systems, such as trapping, tunneling, and thermal detrapping, are not well understood and the experimental demonstration of coherence is often ambiguous.

Fayer and Harris[34] have measured the experimental temperature dependence of the intensity of the intrinsic TCB X trap. If the migration is rapid, equilibration of the triplet state populations can be established among the exciton and trap states within the lifetime of the excited electronic state and the temperature dependence of the trap emission will obey Boltzmann

statistics. If the migration is too slow, equilibrium is not reached and the qualitative behavior of the trap intensity is different. In this study, the experimental results could be fit to a Boltzmann curve with the best possible fit giving a trap concentration of one part in 90,000. This observation can only be interpreted in terms of a model which is dependent upon coherent migration in the TCB crystal at low temperatures.

Table I gives the ratio of the distances travelled by an exciton moving in the coherent limit versus random walk migration at 2.8 K for a narrow band-width excitation (the TCB triplet), a wide band (DBN triplet), and an intermediate band-width. The random walk migration is a factor of 10^4 to 10^6 slower than coherent migration. While a TCB exciton travelling completely coherently could sample approximately 10^9 lattice sites during its lifetime (10 msec), an exciton undergoing random walk migration will only sample about 10^4 lattice sites. The number of such excitons able to migrate longer distances falls off rapidly because one-dimensional random walk processes are describable by a Gaussian distribution of distances about the initial site. In the case of TCB, only three excitons out of 1000 travelling completely incoherently would be able to cover a distance of 5×10^4 lattice sites, which is half the average distance between traps. The conclusion drawn by the authors from the fact that the temperature dependence of the TCB trap intensity obeys Boltzmann statistics is that coherent migration is the principal mode of transport. No estimate of

the actual coherence length is given, although the coherence length must be several orders of magnitude longer than the lattice spacing in order for the system to achieve thermal equilibrium within the excited-state lifetime.

A similar experimental study has been made by Dlott, Fayer, and Wieting.[75] Their kinetic model, however, analyzes the effect of the natural abundance of hd-TCB "barriers" 11 cm^{-1} above the band, assuming coherent propagation between the barriers and an overall stochastic random walk between intervals bounded by barriers. Trap population build-up rates are calculated for individual wave-vector states, including k-dependent group velocities and barrier tunneling rates, before a thermal average over the rates is taken. The coherent model predicts a phosphorescence build-up rate in the TCB X trap that is larger than that measured, although the model for the completely incoherent exciton gives a rate substantially too low. Effects related to intermediate coherence lengths and multidimensional interactions cannot be extracted from the model and no unequivocal statement about coherence can be made.

Shelby, Zewail and Harris[76] observed the time evolution of exciton and trap phosphorescence by exciting the triplet band states of TCB and DBN with nanosecond dye laser pulses. The behavior was fit to a kinetic model whose parameters were the exciton and trap decay rates, the trapping rate, and the detrapping rate. The trapping rate, k_i, was in turn related

to the mode of exciton propagation in the band. In the regime where exciton-phonon coupling decreases the coherence time, but does not completely localize the exciton wavepacket, the trapping rate is described by a random walk with step length ℓ and step time $\langle\tau(k)\rangle$, the average coherence lifetime,

$$k_i = \ell^2/\tau d^2 \qquad (31)$$

where d is the distance between traps. Although the model fits the experimental results quite well the experiment is subject to ambiguity. Güttler and Wolf[77] point out that the trapping efficiency is on the order of 10^{-4} if the ratio of trapping and detrapping rates is determined by microscopic reversibility and the number of band states; thus, the trapping rate may be limited by the final trapping step rather than migration to the region of the trap. It appears at present that no unequivocal statement about coherence can be made on the basis of these experiments.

Coherence studies in multi-dimensional systems have been hampered by the greater complexity of the statistical models necessary to predict the experimental observables. Argyrakis and Kopelman[78] have developed a method of measuring the coherence

length based on exciton percolation in isotopic mixed crystals, a mathematical idealization ofatwo-component system in which energy transfer is only allowed between adjacent, low energy component molecules. Modeling the naphthalene first singlet exciton system with a nearest neighbor interaction and square lattice topology, they generate a binary random lattice of 500 by 500 sites and find the number of sites visited as a function of the exciton mean free path. They relate their results to the experimental results for energy partitioning between the low energy component and a dilute concentration "supertrap" and find that a coherence length of 20-100 sites reproduces the experimental curve best. One needs, however, extremely accurate data to distinguish between 20 and 100 site coherence lengths when the average distance between isotopic scatterers is only 5 to 10 sites.

An additional technique of potential importance in the study of exciton coherence is biexcitonic annihilation and delayed fluorescence. Suna[79] and Gösele[80] have modeled the rate of exciton fusion, particularly in one- and two-dimensional systems, as a function of the exciton diffusion tensor, and the predicted behavior has been observed both in neat and mixed crystal systems[81]. But so far theoretical and experimental work have dealt primarily with incoherent migration at higher temperatures.

SUMMARY

The fundamental concepts of coherent exciton propagation in molecular solids provide a simple relationship between exciton-phonon scattering, spectral lineshape, and exciton migration dynamics and the search for coherence has been an area of active research in the last decade. Three classes of experimental techniques have been used to demonstrate exciton coherence: electron spin resonance, optical lineshapes, and exciton dynamics measurements. Most studies have been made on one-dimensional exciton conductors, where experimental results and theoretical predictions are easily compared, but we see a need to study coherence in a wider range of compounds to show whether or not it is indeed a general property of exciton migration at low temperatures.

References

1. Hochstrasser, R. 1966. Ann. Rev. Phys. Chem. 17:457.
2. Robinson, G. W. 1970. Ann. Rev. Phys. Chem 21:429.
3. Kopelman, R. 1975. in Excited States, Vol 2, ed. E.C. Lim, New York: Academic Press.
4. El-Sayed, M. 1975. Ann. Rev. Phys. Chem. 26:235.
5. Soos, Z. 1974.Ann. Rev. Phys. Chem. 25:121.
6. Silbey, R. 1976. Ann. Rev. Phys. Chem. 27:203.
7. Frenkel, J. 1931. Phys. Rev. 37:13, 1276.
8. Toyozawa, Y. 1958. Prog. Theor. Phys. 20:53.
9. Ibid. 1959. Suppl. 12:111.
10. Onodera, Y. and Toyozawa, Y. 1968. J. Phys. Soc. Japan 24:341.
11. Toyozawa, Y. 1976. J. Luminescence 12:13.
12. Sumi, H. 1974. J. Phys. Soc. Japan 36:770.
13. Sumi, H. 1972. J. Phys. Soc. Japan. 32:616.
14. Suna, A. 1964. Phys. Rev. 135:A111.
15. Harris, C. B. 1977. J. Chem Phys. 67:5607.
16. Harris, C. B. 1977. Chem. Phys. Lett. 52:5.
17. Davydov, A. S. 1971. Theory of Molecular Excitons.New York;Plenum
18. Rashba, E. I. 1957. Opt. Spektrosk 2:568.
    Rashba, E. I. 1963. Sov. Phys-Solid State 4:2417.
19. Schwarzer, E. and Haken, H. 1973. Opt. Comm. 6:64.
20. Philpott, M. 1971. J. Chem. Phys. 55:2039.
21. Thomas, D. and Hopfield, J. 1961. Phys. Rev. 124:657.
22. Francis, A. H. and Harris, C. B. 1971. J. Chem. Phys. 55:3595.
23. Francis, A. H. and Harris, C. B. 1971. Chem. Phys. Lett. 9:181.

24. Ibid, 9:188

25. Gallus, G. and Wolf, H. 1966. Phys. Stat. Sol.16:277.

26. Kepler, R. G. and Switendick, A. E. 1965. Phys. Rev. Lett. 15:56.

27. Avakian, P. and Merrifield, R. 1964. Phys. Rev. Lett. 13:541.

28. Craig, D., Walmsley, C. 1968. Excitons in Molecular Crystals. New York: Benjamin.

29. Zewail, A. H., Harris, C. B. 1975. Phys. Rev. B9:935.

30. Haken, H., Strobl, G. 1968. In the Triplet State, ed.A. Zahlan. Cambridge, Cambridge Univ. Press.

31. Soules, T., Duke, G. 1971. Phys. Rev. B3:262.

32. Rackovsky, S., Silbey, R. 1973. Mol. Phys. 25:61.
Abram, I., Silbey, R. 1975. J. Chem. Phys. 63:2317.

33. Harris, C. B., Fayer, M. D. 1974. Phys. Rev. B 10:1784.

34. Fayer, M. D., Harris, C. B. 1974. Phys. Rev. B9:748.

35. Förster, T. 1948. Ann. Phys. N. Y. 2:55.
Förster, T. 1965. In Modern Quantum Chemistry. Ed. O. Sinanoglu 3:93. New York: Academic.

36. Haken, H., Reinecker, P. 1972. Z. Physik 249:253.

37. Reinecker, P., Haken, H. 1972. Z. Physik 250:300.

38. Schwarzer, E., Haken, H. 1973. Opt. Comm. 9:64.

39. Grover, M., Silbey, R. 1971. J. Chem. Phys. 54:4843.

40. Grover, M., Silbey, R. 1970. J. Chem. Phys. 52:2099.

41. Munn, R. W., Siebrand, W. 1970. J. Chem. Phys 52:47.

42. Kenkre, V., Knox, R. 1974. Phys. Rev. B9:5279.

43. Kenkre, V., Knox, R. 1974. Phys. Rev. Lett. 33:803.

44. Kenkre, V. 1975. Phys. Rev. B11:1741.

45. Ibid, 12:2150

46. Pearlstein, R. 1972. J. Chem. Phys. 56:2431.

47. Lakatos-Lindenberg, K., Hemenger, R., Pearlstein, R. 1972. J. Chem. Phys. 56: 4852.

48. Greer, W. L. 1974. J. Chem. Phys. 60:744.

49. Greer, W. L. 1976. J. Chem. Phys. 65:3510.

50. Zwemer, D. A., Harris, C. B. 1978. To appear in J. Chem. Phys. Feb. 15.

51. Herbstein, F. 1965. Acta Cryst. 18:997.

52. Bloch, F. 1946. Phys. Rev. 70:460.

53. Dlott, D., Fayer, M. D. 1976. Chem. Phys. Lett. 41:305.

54. Lewellyn, M. T., Harris, C. B. unpublished results. Lewellyn, M. T., 1977 Ph.D. Thesis, University of California, Berkeley.

55. Zewail, A. H., Harris, C. B. 1974. Chem. Phys. Lett. 28:8.

56. Zewail, A. H., Harris, C. B. 1975. Phys. Rev. B 11:952.

57. Harris, C. B., Breiland, W. G. 1977. Laser and Coherence Spectroscopy, ed. J. I. Steinfeld, New York: Plenum.

58. Breiland, W. G., Brenner, H. C., Harris, C. B. 1975. J. Chem. Phys. 62:3458.

59. Botter, B. J., Dicker, A.I.M, Schmidt, J. 1978. Chem. Phys. Lett. xx:xxxx

60. Botter, B. J., Nonhof, C. J., J. Schmidt, Van der Waals, J. H. 1976, Chem. Phys. Lett. 43:210.

61. (a) Schmidberger, R., Wolf, H. C. 1972. Chem. Phys. Lett. 16:402 (b) Ibid 1974. 25:185 (c) Ibid. 1975 32:18 (d) Ibid. 1975 32:21.

62. Haken, H., Strobl, T. 1973. Z. Physik 262:135.

63. Brewer, R. G. Genack, A. Z. 1976. Phys. Rev. Lett. 36:959. Aartsma, T., Wiersma, D. 1976. Phys. Rev. Letters. 36:1360. Morsink, J., Aartsma, T., Wiersma, D. 1977. Chem. Phys. Lett. 49: 34.
Zewail, A. H., Orlowski, T. E., Jones, K. E. 1977. Proc. Natl. Acad. Sci. USA. 74:1310.

64. Burland, D. M., Cooper, D. E., Fayer, M. D., Gochanour, C.R. 1977. Chem. Phys. Lett. 52:279.

65. Morris, T., Sceats, M. 1973. Chem. Phys. 1:120.

66. Ibid,1974. 3:332.

67. Ibid, 342.

68. Sumi, H. 1975. J. Phys. Soc. Japan. 38: 825.
Soven, P. 1967. Phys. Rev. 156:809.

69. Anderson, P. W. 1954. J. Phys. Soc. Japan. 9:316.

70. Kubo, R. 1954. J. Phys. Soc. Japan. 9:935.
Kubo, R., Tomita, K. 1954. J. Phys. Soc. Japan 9:888.

71. Swift, T. J., Connick, R. E. 1962. J. Chem. Phys. 37:307.

72. Van't Hof, C. A., Schmidt, J. 1975. Chem. Phys. Lett. 36:457.

73. Burland, D. M. 1973. J. Chem. Phys. 59:4283.

74. Burland, D. M., Konzelmann, U., Macfarlane, R. M. 1977. J. Chem. Phys. 67:1926.

75. Dlott, D. D., Fayer, M. D., Wieting, R. D., 1977. J. Chem. Phys. 67:3808.

76. Shelby, R. M., Zewail, A. H., Harris, C. B. 1976. J. Chem. Phys. 64:3192.

77. Güttler, W., Von Schutz, J. U., Wolf, H. C. 1977. Chem. Phys. 24:159.

78. Argyrakis, P., Kopelman, R. 1977. J. Chem. Phys. 66:3301.

79. Suna, A. 1970. Phys. Rev. B1:1716.

80. Gösele, U. 1976. Chem. Phys. Lett. 43:61.

81. Ern, V., Suna, A., Tomkiewicz, Y., Avakian, P., Groff, R. 1972. Phys. Rev. B5:3222.
Ern, V., Bouchriha, H., Schott, M., Castro, G. 1974. Chem. Phys. Lett. 29:453.

Table I. Ratio of the Coherent Migration Distance to the Random walk distance at 2.8 K.

Time	Band Width		
	1.25 cm^{-1}	15 cm^{-1}	29.6 cm^{-1}
1 ms	3.7×10^4	7.8×10^4	7.8×10^4
10 ms	1.1×10^5	2.5×10^5	2.5×10^5
100 ms	3.7×10^5	7.8×10^5	7.8×10^5
1 s	1.1×10^6	2.5×10^6	2.5×10^6

Figure Captions

Figure 1: The relationship between the translationally equivalent interaction, β, the band energy dispersion, $E(k)$, the group velocity, $V_g(k)$, the density of states function, $\rho(E)$, and the distribution function $D(k)$, for a one-dimensional exciton.

Figure 2: Stacking pattern for two inequivalent chains in 1,2,4,5 - tetrachlorobenzene. Center to center distance along $\vec{a}$ axis (left-right in plane of paper) is 3.76Å.

Figure 3: Coherent properties of electronically excited dimers.

Figure 4: Expected Larmor frequencies for one-dimensional systems. $\omega(M)$ is the Larmor frequency of two spin sublevels, T_x, T_y, of the excited triplet state. $\omega(+)$ and $\omega(-)$ are the two different frequencies in $\psi(+)$ and $\psi(-)$ dimer states. $\omega(k=0)$, $(k=\pi/a)$, and $\omega(k=\pi/2a)$ are the Larmor frequencies of $k=0$, $k=\pi/a$ (band edges) and $k=\pi/2a$ (band center) states, respectively. Extraction of the Larmor frequency for any other k-state from the schematic is straight forward. The right hand side of the figure demonstrates the effect of exchange on the microwave absorption in dimer and exciton states.

(a) the isolated molecule transition.

(b) Microwave absorption in dimers for a slow exchange limit; Δ_k is the difference in Larmor frequencies of $\psi(+)$ and $\psi(-)$ states.

(c) Microwave absorption in dimers for a fast exchange limit. Both $\omega(+)$ and $\omega(-)$ are centered around (M).

(d) Exciton band-to-band transition extrapolated from the dimer case "b" in the slow exchange limit. Δ_k is directly related to Δ_k.

(e) Exciton resonance in the fast exchange limit. $\omega(k)$ is centered around $\omega(M)$.

Figure 5: The optically detected $D + |E|$ (top) and $D - |E|$ (bottom) band-to-band transitions associated with the triplet exciton in 1,2,4,5-tetrachlorobenzene. The phosphorescence

intensity of the exciton electronic origin at 3748.2Å is monitored as a function of microwave frequency. The solid line is the theoretically predicted spectra of Francis and Harris[25].

Figure 6: The right hand section of this figure demonstrates the relationship between exciton and dimer microwave dispersions in coherent states. The energy dispersion of the band is one-dimensional. The dashed lines represent the position of the dimer and monomer energies, E ($\pm$) and E (M), in the band and their relationship to the microwave resonance frequencies, $\omega(\pm)$ and ω(M). The spectra on the left are the microwave band-to-band transitions taken from ref. (25). The dashed vertical bars represent the experimental frequencies of the dimer in the D + |E| and D - |E| transitions[55,56] and the width of these bars is the estimated error on these frequencies.

COHERENT PROPERTIES OF EXCITONS

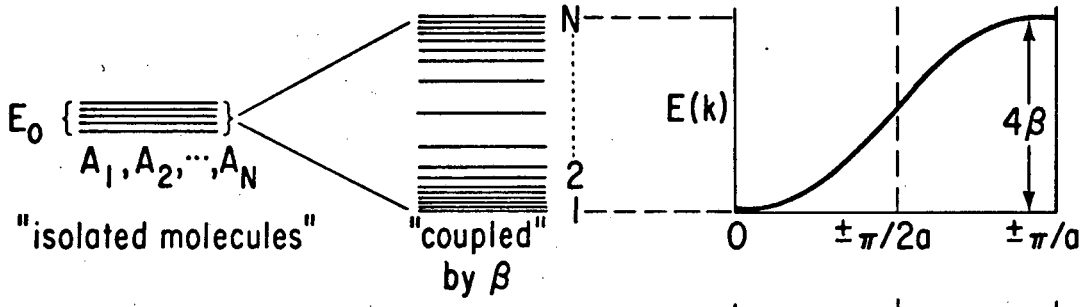

1. β generates a rate of energy transfer between molecules: $\nu_g(k)$.
2. Coherence lifetime, $\tau(k)$, generates a width to the state *and* a mean-free path for coherent energy migration

$$\ell(k) = \nu_g(k) \cdot \tau(k)$$

$$\tau(k)^{-1} \equiv \sum_{k'} (\tau_{kk'})^{-1} = \Gamma(k)$$

3. Distribution Function, D(k), determines the partition of energy between states of different velocities

$$D(k)_B \sim \rho(k) \exp[-E(k)/kT]$$

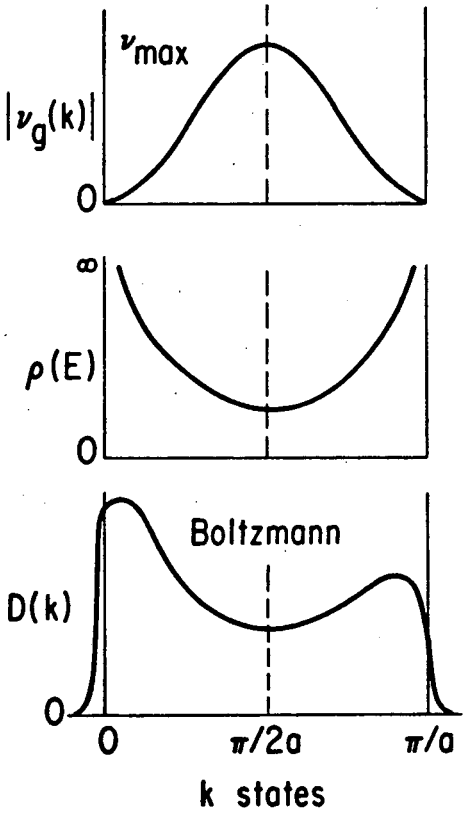

XBL 734-394

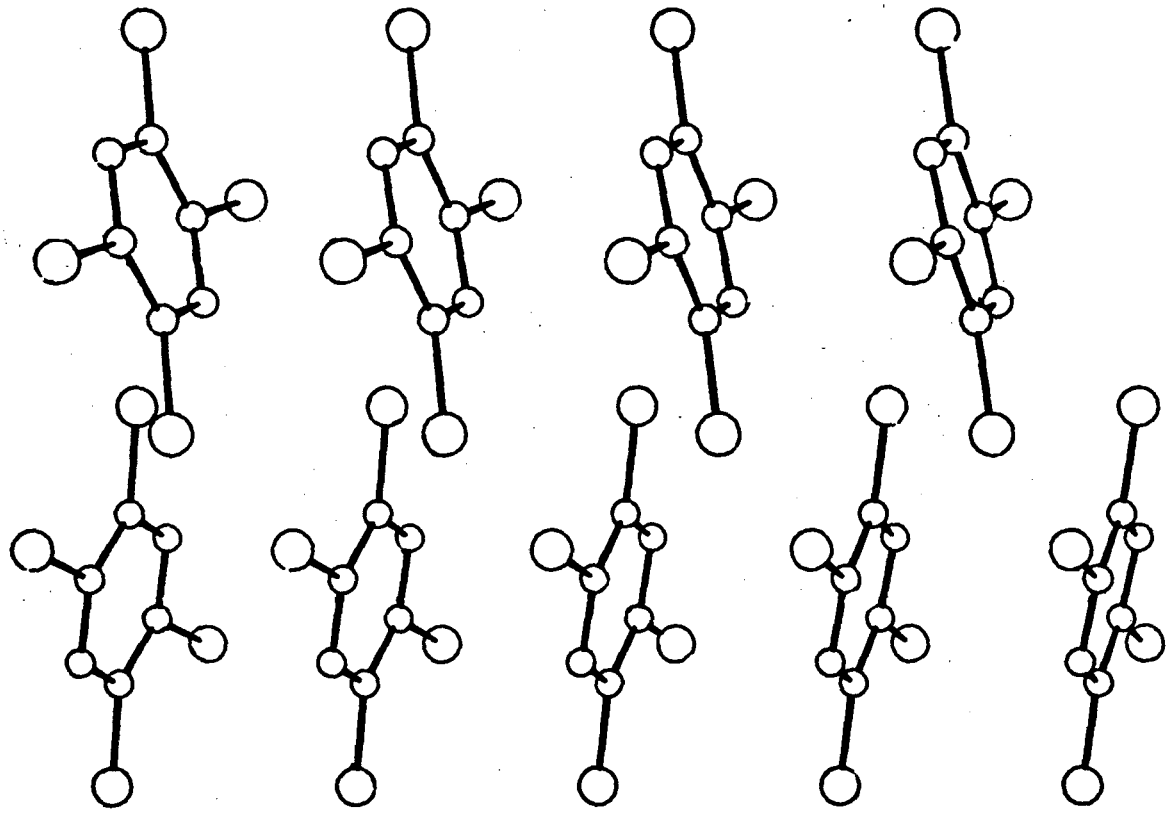

1,2,4,5-Tetrachlorobenzene

XBL 734-398

COHERENT PROPERTIES OF DIMERS

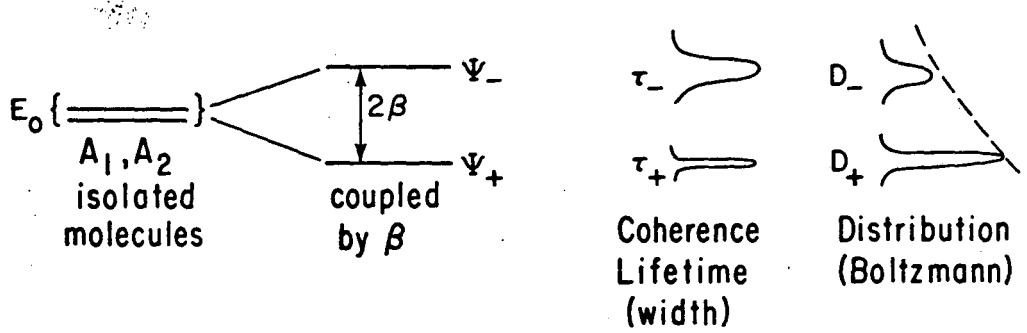

(1) β generates a rate of energy transfer between molecules:

$$\nu_+ = \nu_- = 2\beta$$

(2) Coherence lifetime, τ_+ or τ_-, generates a width to the state and is a measure of the coupling of the dimer to its environment.

$$[\tau_+^{-1} = \sum_i (\tau_{+i})^{-1};\ \tau_-^{-1} = \sum_i (\tau_{-i})^{-1}]$$

(3) Distribution function, D, determines the partition of energy between Ψ_+ and Ψ_-.

$$[D_- \sim D_+ \cdot \exp(-2\beta/kT) \cdot \Gamma_-]$$

XBL 734-392

EXPECTED LARMOR FREQUENCIES FOR DIMERS AND EXCITONS OF ONE-DIMENSIONAL CRYSTALS
IN THE SLOW AND FAST EXCHANGE LIMITS

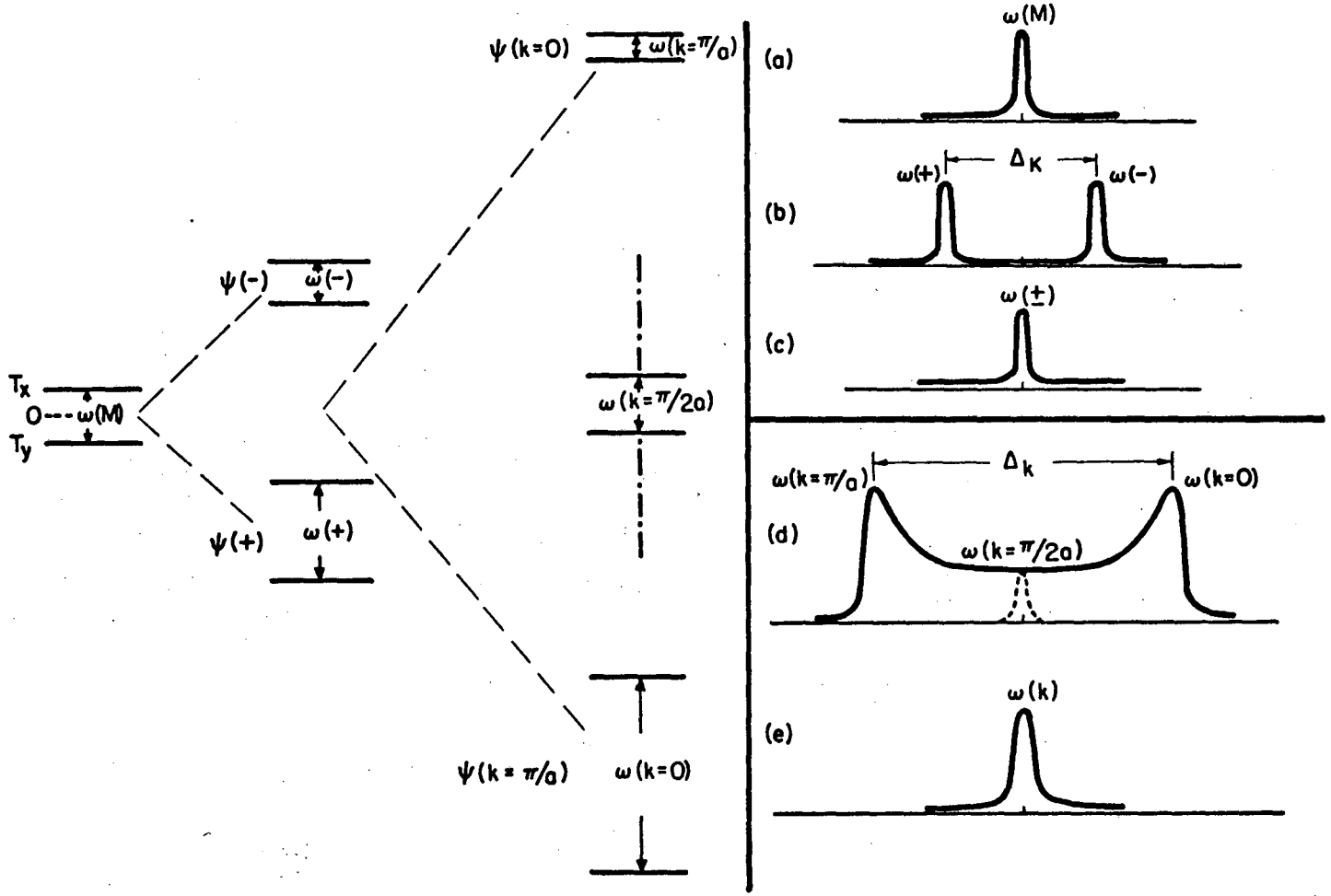

XBL747-6803

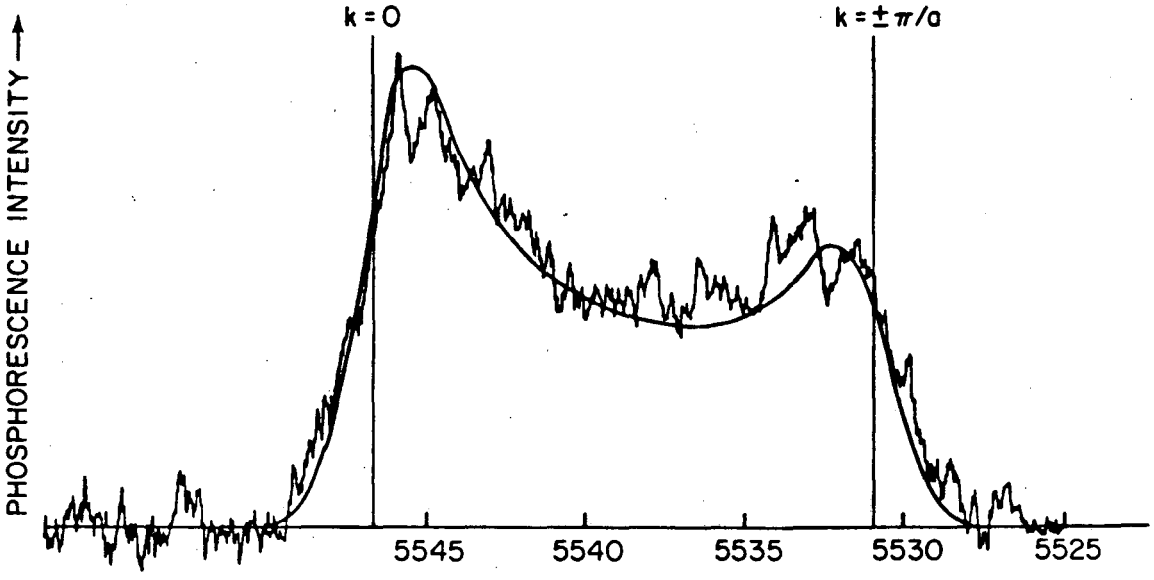
k = 0
k = ± π/a
PHOSPHORESCENCE INTENSITY
5545
5540
5535
5530
5525

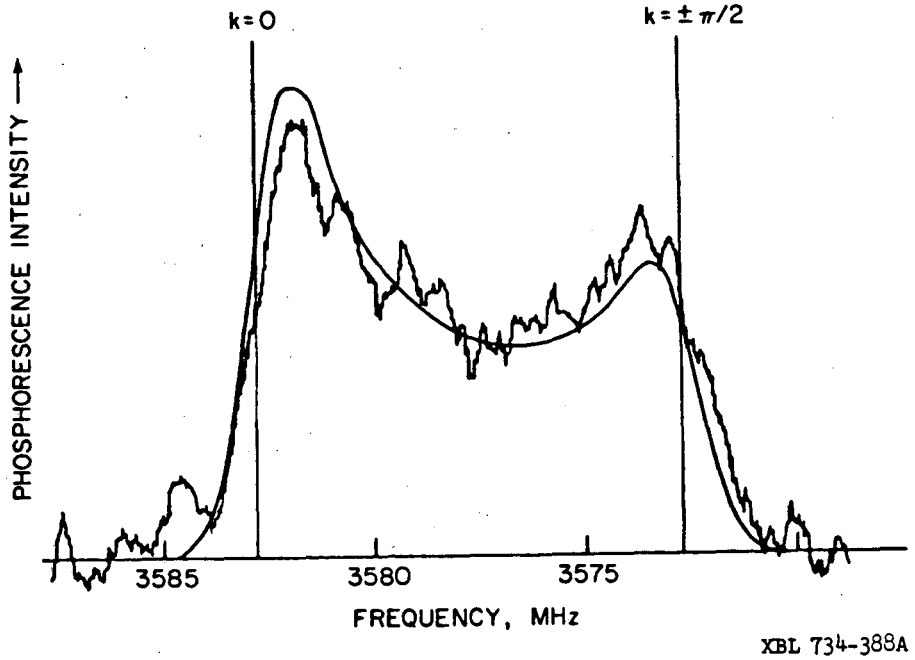
k=0
k = ± π/2
PHOSPHORESCENCE INTENSITY
3585
3580
3575
FREQUENCY, MHz

XBL 734-388A

THE RELATIONSHIP BETWEEN EXCITON AND DIMER MICROWAVE DISPERSIONS IN COHERENT STATES AND THE EXPERIMENTAL RESULTS ON 1, 2, 4, 5 - TETRACHLOROBENZENE

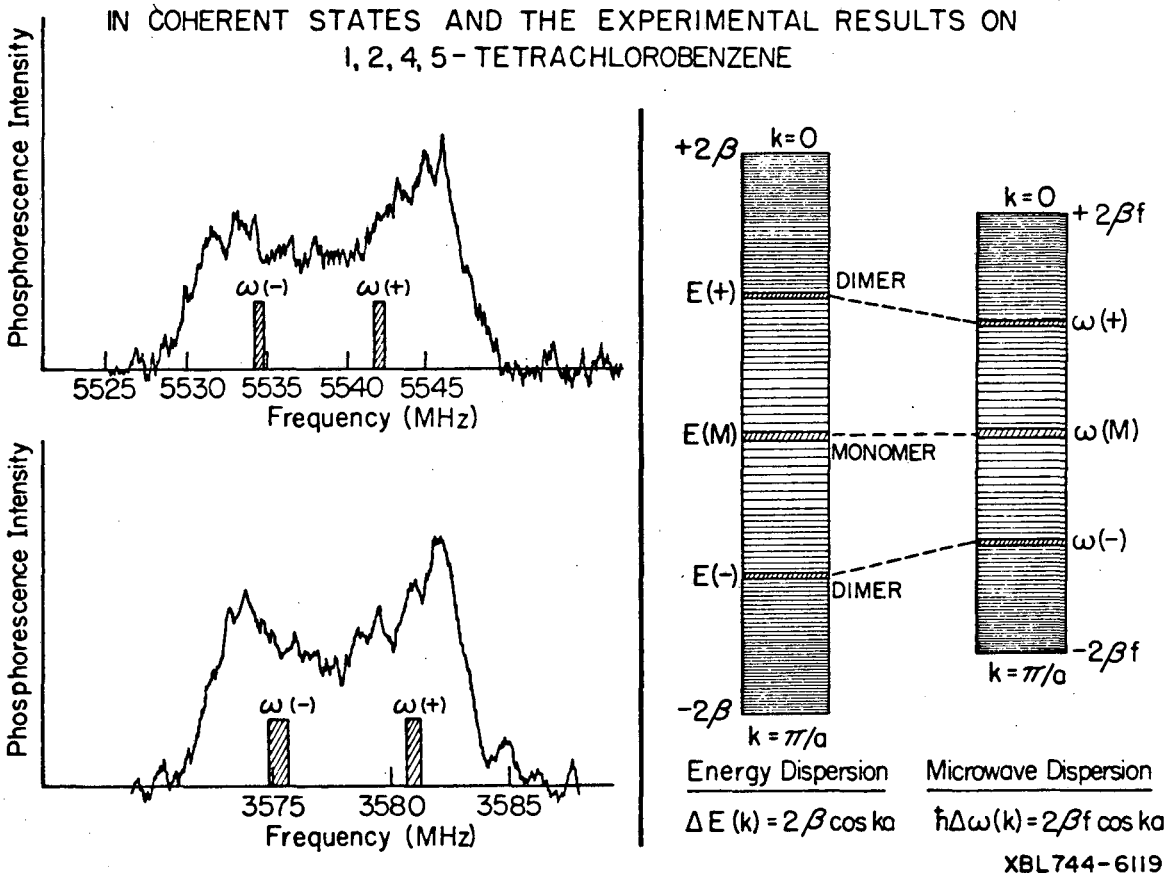

XBL744-6119

TECHNICAL INFORMATION DEPARTMENT
LAWRENCE BERKELEY LABORATORY
UNIVERSITY OF CALIFORNIA
BERKELEY, CALIFORNIA 94720